Synthesis, Folding, and Association of Long Multiblock $(PEO_{23}$-*b*-$PNIPAM_{124})_{750}$ Chains in Aqueous Solutions

Qingwei Zhang,[†] Jing Ye,[‡] Yijie Lu,[§] Ting Nie,[†] Dinghai Xie,[§] Qiliang Song,[§] Hongwei Chen,[§] Guangzhao Zhang,[§] Yong Tang,[†] Chi Wu,*[,‡,§] and Zuowei Xie*[,†,‡]

The Shanghai-Hong Kong Joint Laboratory in Chemical Synthesis, Shanghai Institute of Organic Chemistry, The Chinese Academy of Sciences, Shanghai 200032, China; Department of Chemistry, The Chinese University of Hong Kong, Shatin, N.T., Hong Kong; and The National Laboratory of Physical Science at Microscale, Department of Chemical Physics, University of Science and Technology of China, Hefei, Anhui 230026, China

Received September 25, 2007; Revised Manuscript Received January 7, 2008

ABSTRACT: A thermally sensitive ultralong multiblock copolymer, [poly(ethylene oxide)$_{23}$-*b*-poly(*N*-isopropylacrylamide)$_{124}$]$_{750}$ ($M_w = 1.78 \times 10^7$ g/mol and $M_z/M_w = 1.49$), was prepared using the oxidative coupling of two mercapto groups at the two ends of triblock $PNIPAM_{62}$-*b*-PEO_{23}-*b*-$PNIPAM_{62}$ ($M_{n,PEO} = 1.0 \times 10^3$ g/mol and $M_{n,PNIPAM} = 1.4 \times 10^4$ g/mol) copolymer chains. The folding of individual multiblock copolymer chains in an extremely dilute solution (10^{-6} g/mL) was studied by laser light scattering (LLS). Moreover, the association of multiblock and triblock copolymer chains in relatively concentrated aqueous solutions (10^{-3} g/mL) was also comparatively studied by a combination of LLS, fluorescence spectrometry, and microcalorimetry. We found that in the single-chain folding process the average radius of gyration ($\langle R_g \rangle$) remains a constant in one heating-and-cooling cycle, but the average hydrodynamic radius ($\langle R_h \rangle$) decreases as the solution temperature increases. Our result reveals that the single-chain folding undergoes two stages at ~32 and ~40 °C, presumably due to the successive contraction of thermally sensitive PNIPAM segments in the middle around each hydrophobic S−S coupling point and near the hydrophilic PEO block. Each PNIPAM block collapses into a small globule (bead) stabilized by the two attached PEO blocks on the chain backbone, a string−bead conformation, which makes the chain thicker and more extended. The association of multiblock chains also undergoes similar two stages to form stable mesoglobules during the heating. In contrast, the triblock chains associate at ~30 °C to form polymeric micelles.

Introduction

Since Lifshitz[1] stated that the level of biological structural hierarchy of biopolymers can lead to their related physical properties, single-chain folding has been extensively studied.[2] Protein chains generally contain hydrophobic and hydrophilic charged or noncharged amino acid residues, regarded as amphiphilic copolymers in a broad definition. The coordinate and cooperative interactions, such as intra- and interchain hydrogen bonding, hydrophobic attraction, and electrostatic attraction/repulsion, led to some complicated bioactive structures.[3] To simplify such a complicated problem, polymer researchers have tried to prepare protein-like amphiphilic copolymer chains made of hydrophilic and hydrophobic monomers with different structures to imitate protein chains.[4−12] It is anticipated that the folding of these simplified amphiphilic copolymer chains could shed some light on the complicated protein folding.

Khokholv et al.[4] simulated three types of AB copolymer chains with an identical composition and length, but different comonomer distributions on the chain backbone. Their results show that the folding of a copolymer chain with a protein-like structure, i.e., soluble comonomer A was incorporated on the periphery of collapsed B segments, is easier and the resultant globule is more stable and denser than that from a random copolymer chain. The simulation results suggest that such a protein-like chain can memorize or inherit some special functional properties of its parent collapsed state. Timoshenko et al.[5] also showed that for a given degree of amphiphilicity the folding of AB copolymer chains with a segmented comonomer distribution was easier than a random copolymer chain, leading to stable mesoglobules in comparison with random copolymer chains under the same conditions. However, it is an experimental challenge to prepare a pair of AB copolymers with a similar composition and chain length, but different comonomer distributions on the backbone.

We have been interested in this kind of problems for many years and attempted to synthesize regular $(AB)_n$ multiblock copolymers with a controllable block length and sequence for the investigation of the chain folding and other related problems.[2] In the preparation of these amphiphilic copolymers, poly(*N*-isopropylacrylamide) (PNIPAM) with a convenient low critical solution temperature (LCST ~32 °C) in water is a favorable choice as one component.[13] It is this interesting thermal property that has made PNIPAM a model polymer for the study of protein denaturalization in aqueous solutions even though protein chains are much more complicated.[14] We also note that water is a good solvent for poly(ethyl oxide) (PEO) in the temperature range 20−50 °C. Therefore, a copolymer made of PNIPAM and PEO is soluble at lower temperatures (~32 °C) but becomes amphiphilic at higher temperatures. In this study, we first synthesized a PNIPAM-*b*-PEO-*b*-PNIPAM triblock copolymer with two SH ends via reversible addition−fragmentation chain transfer (RAFT) polymerization.[15,16] The multiblock $(PEO$-*b*-$PNIPAM)_n$ copolymer was then obtained via the oxidative coupling of every two SH ends on different triblock

* The Hong Kong address should be used for all correspondence.
† The Chinese Academy of Sciences.
‡ The Chinese University of Hong Kong.
§ University of Science and Technology of China.

10.1021/ma702139b CCC: $40.75
Published on Web 02/19/2008

copolymer chains. The folding of individual multiblock copolymer chains in an extremely dilute solution and the comparison of association of triblock and multiblock copolymer chains in relatively more concentrated solutions were studied.

Experimental Section

Materials and Sample Preparation. All chemicals, unless otherwise specified, were purchased from Aldrich Chemical Co. *S*-1-Dodecyl-*S*′-(α,α′-dimethyl-α″-acetic acid) trithiocarbonate was prepared according to the literature method.[17] THF and toluene (99%) were refluxed several hours and freshly distilled from sodium benzophenone ketyl immediately prior to use. Azobis(isobutyronitrile) (AIBN, 97%) was recrystallized three times from methanol. *N*-Isopropylacrylamide (97%) was recrystallized twice from a solution of hexane/toluene (1:1). ^{1}H NMR spectra were recorded on a Bruker AM-300 spectrometer. Chemical shifts were reported in δ units with reference to internal or external TMS (0.03% v/v). From the number-average molar mass of individual PEO blocks, the number-average molar mass of triblock PNIPAM-*b*-PEO-*b*-PNIPAM copolymer was estimated by ^{1}H NMR spectra. The polydispersity index (PDI) of triblock copolymer chains was measured by a Waters 515 gel permeation chromatograph (GPC) equipped with microstyragel columns. THF was used as eluent at a flow rate of 1.0 mL/min.

PEO Macromolecular RAFT Reagent. A CH_2Cl_2 (20 mL) solution containing PEO (M_n = 1000) (0.50 g, 1.0 mmol OH) and dicyclohexylcarbodiimide (DCC) (0.27 g, 1.3 mmol) was added dropwise to a solution of *S*-1-dodecyl-*S*′-(α,α′-dimethyl-α″-acetic acid) trithiocarbonate (0.47 g, 1.3 mmol) and 4-(dimethylamino)-pyridine (DMAP) (0.03 g, 0.25 mmol) in CH_2Cl_2 (20 mL) at room temperature. After the mixture was stirred for 10 h at room temperature, the precipitate of 1,3-dicyclohexylurea (DCU) was filtered off, and the filtrate was evaporated to dryness. The residue was extracted with acetone (10 mL × 3). Removal of the solvent gave a crude product which was purified by fast column chromatography on silica (SiO_2) using methanol as eluent. Yield: 0.72 g (85%). ^{1}H NMR ($CDCl_3$, ppm): δ 0.90−2.00 (m, $-C_{11}H_{23}$, $O{=}C(CH_3)_2$), 3.27 (t, $-CH_2S$), 3.65 (s, $-CH_2O$), 4.26 (t, $-CH_2-O-C{=}O$).

$C_{12}H_{25}SC(=S)S-PNIPAM_{62}$-*b*-$PEO_{23}$-*b*-$PNIPAM_{62}-SC(=S)SC_{12}H_{25}$. A Schlenk tube was charged with PEO macromolecular initiator (0.60 g, 0.35 mmol), NIPAM (2.00 g, 17.7 mmol), and AIBN (0.06 g, 0.35 mmol) in a mixture of toluene and 1,4-dioxane (40 mL, v/v = 1:1). It was then degassed by three freeze−evacuate−thaw cycles, and the polymerization was carried out at 70 °C for 6 h. The tube was immediately immersed into liquid nitrogen for 0.5 h. $C_{12}H_{25}SC(=S)S-PNIPAM_{62}$-*b*-$PEO_{23}$-*b*-$PNIPAM_{62}-SC(=S)S-C_{12}H_{25}$ triblock copolymer was collected after addition of absolute diethyl ether (500 mL). Yield: 2.00 g (85%). M_n: 15 000 (from ^{1}H NMR) and PDI: 1.13 (by GPC). ^{1}H NMR ($CDCl_3$, ppm): δ 1.17 (s, $-CH_3$), 1.20−2.50 (m, $-CH_2-CH$), 3.65 (s, $-CH_2O$), 4.00 (s, $-CH(CH_3)_2$). UV (THF): λ_{max} = 310 nm.

$NC(Me_2)C-PNIPAM_{62}$-*b*-PEO_{23}-*b*-$PNIPAM_{62}-C(Me_2)CN$. A Schlenk tube was charged with $C_{12}H_{25}SC(=S)S-PNIPAM_{62}$-*b*-$PEO_{23}$-*b*-$PNIPAM_{62}-SC(=S)SC_{12}H_{25}$ triblock copolymer (0.32 g, 0.02 mmol) and AIBN (0.24 g, 1.4 mmol) in a mixture of toluene and 1,4-dioxane (20 mL, v/v = 1:1). It was then degassed by freeze−evacuate−thaw cycles, and reaction was carried out at 70 °C for 3 h. $NC(Me_2)C-PNIPAM_{62}$-*b*-PEO_{23}-*b*-$PNIPAM_{62}-C(Me_2)CN$ triblock copolymer was collected after addition of absolute diethyl ether (250 mL). Yield: 0.15 g (47%). ^{1}H NMR ($CDCl_3$, ppm): δ 1.17 (s, $-CH_3$), 1.20−2.80 (m, $-CH_2-CH$), 3.65 (s, $-CH_2O$), 4.00 (s, $-CH(CH_3)_2$). PDI: 1.19. UV: the peak of trithiocarbonate at 310 nm was disappeared.

Multiblock Copolymer (PEO_{23}-*b*-$PNIPAM_{124})_{750}$. A Schlenk tube was charged with triblock copolymer, $C_{12}H_{25}SC(=S)S-PNIPAM_{62}$-*b*-$PEO_{23}$-*b*-$PNIPAM_{62}-SC(=S)SC_{12}H_{25}$ (0.50 g), in THF (2 mL). The solution was then degassed by three freeze−evacuate−thaw cycles. After addition of ethylenediamine (1.5 mL), the mixture was stirred for 3 h at room temperature before it was poured into anhydrous diethyl ether (20 mL) under argon. The precipitate ($HS-PNIPAM_{62}$-*b*-PEO_{23}-*b*-$PNIPAM_{62}-SH$) was collected and dissolved in distilled water, to which oxygen was bubbled for 48 h at room temperature. The polymer solution was purified by dialysis (with cutoff 16 000) using a large amount of water. The final product was dried under vacuum at 40 °C. Yield: 0.20 g (40%). ^{1}H NMR ($CDCl_3$, ppm): δ 1.17 (s, $-CH_3$), 1.20−2.50 (m, $-CH_2-CH$), 3.65 (s, $-CH_2O$), 4.00 (s, $-CH(CH_3)_2$). M_w = 1.78 × 10^7 g/mol and PDI = 1.49 from LLS.

It should be noted that there are only two reactive end groups on each initial triblock chain so that no gel can be formed in such a coupling reaction. On the other hand, it is well-known that the formation of cyclic chains is rather difficult in such a relatively concentrated solution. The probability of cyclic reaction (self-coupling) should be very low, if any.

Laser Light Scattering. A commercial LLS spectrometer (ALV/DLS/SLS-5022F) equipped with a multi-tau digital time correlation (ALV5000) and a cylindrical 22 mW He−Ne laser (λ_0 = 632 nm, UNIPHASE) as the light source was used. In static LLS,[18] we can obtain the weight-average molar mass (M_w), the second virial coefficient (A_2), and the *z*-average root-mean-square radius of gyration ($\langle R_g^2\rangle^{1/2}$ or written as $\langle R_g\rangle$) of scattering objects in a dilute solution or dispersion from the angular dependence of the excess scattering intensity, known as Rayleigh ratio $R_{vv}(q)$, as

$$\frac{KC}{R_{vv}(q)} \approx \frac{1}{M_w}\left(1 + \frac{1}{3}\langle R_g^2\rangle q^2\right) + 2A_2C \quad \text{for } q\langle R_g\rangle \le 1 \text{ (Zimm plot)} \quad (1)$$

or

$$KC/R_{vv}(q) \cong M_w \exp[q^2\langle R_g\rangle^2/3] \quad \text{for } q\langle R_g\rangle > 1 \text{ (Guinier plot)} \quad (2)$$

where $K = 4\pi n^2(dn/dC)^2/(N_A\lambda_0^4)$ and $q = (4\pi n/\lambda_0)\sin(\theta/2)$ with N_A, dn/dC, n, and λ_0 being the Avogadro number, the specific refractive index increment, the solvent refractive index, and the wavelength of the light in a vacuum, respectively. In the chain-folding study, the solution was so dilute that the extrapolation of $C \to 0$ was not necessary; i.e., the second term $2A_2C$ in eq 1 can be dropped. In dynamic LLS,[19] the Laplace inversion (the CONTIN method in the correlator) of each measured intensity−intensity time correlation function $G^{(2)}(q,t)$ in the self-beating mode can lead to a characteristic line-width distribution $G(\Gamma)$. For a diffusive relaxation, Γ is related to the translational diffusion coefficient D by $(\Gamma/q^2)_{C\to0,q\to0} \to D$. Therefore, $G(\Gamma)$ can be converted to a transitional diffusion coefficient distribution $G(D)$ or further to a hydrodynamic radius distribution $f(R_h)$ via the Stokes−Einstein equation, $R_h = (k_BT/6\pi\eta)/D$, where k_B, T, and η are the Boltzmann constant, the absolute temperature, and the solvent viscosity, respectively. In this study, we measured the value of $\langle\Gamma\rangle$ at different scattering angles at each temperature. The extrapolation of $\langle\Gamma\rangle$ to $q \to 0$ led to $\langle D\rangle_0$ and $\langle R_h\rangle$. The solutions were clarified with 0.45 μm Millipore Millex-LCR filters to remove dust.

Micro-DSC and Fluorescence Measurements. The heat flow of each copolymer solution during the phase transition was measured using a VP-DSC microcalorimeter (MicroCal Inc.) at an external pressure of ∼180 kPa. The cell volume was 0.157 mL. The instrument response time was set at 5.6 s. All the micro-DSC data were corrected for the instrument response time and analyzed using the software in the calorimeter. The polymer concentration used in DSC was kept at 1.0 mg/mL, much higher than those used in LLS because of the signal-to-noise ratio. Steady-state fluorescence spectra were recorded on a Varian Cary Eclipse spectrometer at different temperatures. The temperature was maintained by using a water-jacketed cell holder connected to a Cary circulating water bath. The solution temperature of the sample fluid was measured with a thermocouple immersed in a water-filled cell placed in one of the four cell holders in the sample compartment.

Results and Discussion

Synthesis. The RAFT reagent, macromonomer [$C_{12}H_{25}SC(=S)SC(CH_3)_2C(O)O-PEOOC(O)-C(CH_3)_2SC(=S)$-

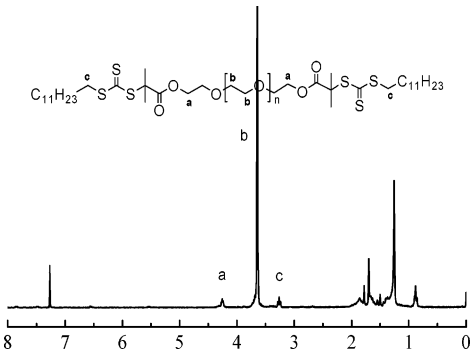

Figure 1. ^{1}H NMR spectrum of PEO macro-RAFT agent in $CDCl_3$.

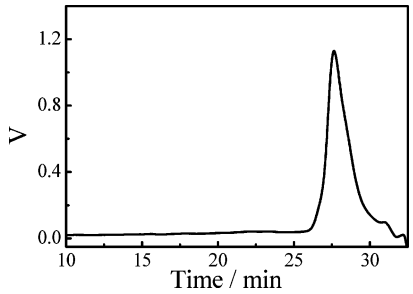

Figure 2. GPC trace (RI detector) of $C_{12}H_{25}SC(=S)S-PNIPAM_{62}$-*b*-$PEO_{23}$-*b*-$PNIPAM_{62}-SC(=S)S-C_{12}H_{25}$ triblock copolymer.

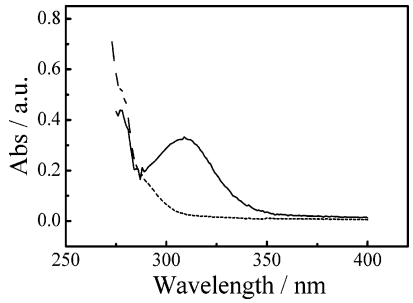

Figure 3. UV spectra of $C_{12}H_{25}SC(=S)S-PNIPAM_{62}$-*b*-$PEO_{23}$-*b*-$PNIPAM_{62}-SC(=S)S-C_{12}H_{25}$ (solid line) and $NC(Me_2)C-PNIPAM_{62}$-*b*-PEO_{23}-*b*-$PNIPAM_{62}-C(Me_2)CN$ (broken line) in tetrahydrofuran.

$SC_{12}H_{25}$] (**1**) was synthesized in 85% isolated yield via the reaction of HO(PEO)OH with 1.3 equiv of *S*-1-dodecyl-*S*′-(α,α′-dimethyl-α″-acetic acid) trithiocarbonate in CH_2Cl_2 in the presence of DCC and DMAP. It was purified by fast column chromatography on silica (SiO_2) using methanol as an eluent. The ^{1}H NMR spectrum of **1** is shown in Figure 1. The peak "a" at 4.25 ppm is assigned to the ester methylene protons $COOCH_2$, and the peak "c" at 3.27 ppm is attributed to the trithiocarbonate methylene protons $CSSCH_2$. The molar ratio of the two peaks is 1:1, indicating a quantitative capping efficiency. The triblock copolymer $C_{12}H_{25}SC(=S)S-PNIPAM_{62}$-*b*-$PEO_{23}$-*b*-$PNIPAM_{62}-SC(=S)SC_{12}H_{25}$ was prepared via RAFT polymerization of NIPAM using **1** as a macrotransfer agent. Its number-average molar mass (M_n) is 16 000 g/mol as determined by ^{1}H NMR using the literature method.[20] The polydispersity index (PDI, M_w/M_n) is ~1.1 measured by GPC (Figure 2). On the other hand, $NC(Me_2)C-PNIPAM_{62}$-*b*-PEO_{23}-*b*-$PNIPAM_{62}-C(Me_2)CN$triblock copolymer was obtained by treatment of $C_{12}H_{25}SC(=S)S-PNIPAM_{62}$-*b*-$PEO_{23}$-*b*-$PNIPAM_{62}-SC(=S)SC_{12}H_{25}$ with a large excess amount of AIBN according to the literature method.[21a] The UV spectrum (Figure 3) shows that the trithiocarbonate peak at 310 nm disappears after the AIBN treatment, supporting the formation of target copolymer.[22]

Scheme 1. Synthesis of Thermally Sensitive Multiblock Copolymer Chains

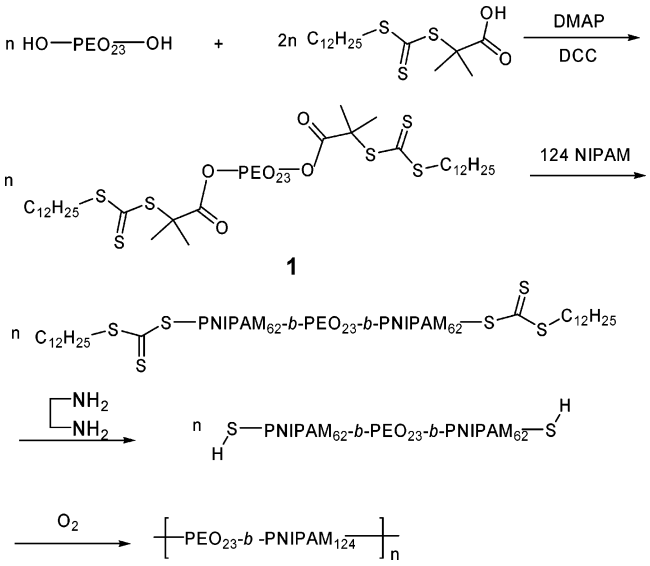

Triblock copolymer $C_{12}H_{25}SC(=S)S-PNIPAM_{62}$-*b*-$PEO_{23}$-*b*-$PNIPAM_{62}-SC(=S)SC_{12}H_{25}$ was easily converted to $HS-PNIPAM_{62}$-*b*-PEO_{23}-*b*-$PNIPAM_{62}-SH$ by reaction with ethylenediamine in THF at room temperature using the literature method.[21b] Oxidative coupling of the two SH end groups on different chains under oxygen gave the target multiblock copolymer $(PEO_{23}$-*b*-$PNIPAM_{124})_n$ (Scheme 1). The polymer was then purified by dialysis (with cutoff 16 000) using a large amount of water to remove short multiblock copolymers. The final product was dried under vacuum at 40 °C. LLS characterization shows that M_w, $\langle R_g\rangle$, $\langle R_h\rangle$, and M_z/M_w of such an obtained multiblock copolymer are 1.78×10^7 g/mol, 103 nm, 100 nm, and 1.49, respectively. It is helpful to note that GPC is not a proper method to characterize such a multiblock copolymer because of its high molar mass. M_z/M_w was estimated using $M_z/M_w = 1 + (1/\nu)^2\mu_2/\langle\Gamma\rangle^2$, where ν and $m_2/\langle\Gamma\rangle^2$ are the Flory exponent (0.5−0.6) and the relative width of the linewidth distribution, respectively. On average, each multiblock chain contains ~750 initial triblock copolymer chains. It is denoted as $(PEO_{23}$-*b*-$PNIPAM_{124})_{750}$ hereafter.

Single-Chain Folding of $(PEO_{23}$-*b*-$PNIPAM_{124})_{750}$ in a Dilute Solution. The copolymer concentration used here was 1.0×10^{-6} g/mL. Figure 4 shows that the slope of $[KC/R_{vv}(q)]$ vs q^2 is independent of the solution temperature. On the basis of eq 1 (experimental section), the intercept at $q \to 0$ and the slope are related to M_w and $\langle R_g\rangle$, respectively. The extrapolation of $KC/R_{vv}(q)$ to $q \to 0$ at three different temperatures leads to the same intercept, indicating there is no change in the weight-average molar mass (M_w), i.e., no interchain association, during the heating process. Note that the value of d*n*/d*C* only weakly depends on the solution temperature. Such a small change slightly affects the measured weight-average molar mass but has no effect on $\langle R_g\rangle$. It has been known that PNIPAM is thermally sensitive in water, and its conformation changes from a random coil to a collapsed globule when the solution is heated to a temperature higher than ~32 °C. Therefore, it is really a surprise to see that $\langle R_g\rangle$ of the multiblock copolymer chains is nearly independent of the solution temperature.

Figure 5 shows the temperature dependence of weight-average molar mass (M_w) of multiblock copolymer chains during one heating-and-cooling cycle. M_w nearly remains a constant, indicating a single-chain process during the heating process. Presumably, each collapsed PNIPAM block (globule) is stabi-

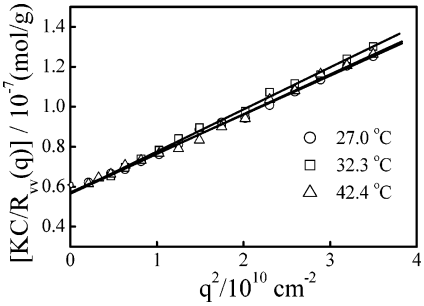

Figure 4. Scattering vector (q) dependence of Raleigh ratio $R_{vv}(q)$ of multiblock copolymer chains in water, where the multiblock copolymer concentration was 1.0×10^{-6} g/mL, and the relative error is no more than 5% for each data point.

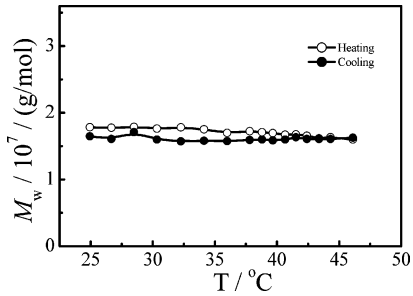

Figure 5. Weight-average molar mass of multiblock copolymer chains as a function of the temperature at the concentration of 1.0×10^{-6} g/mL, where the relative error is no more than 5% for each data point.

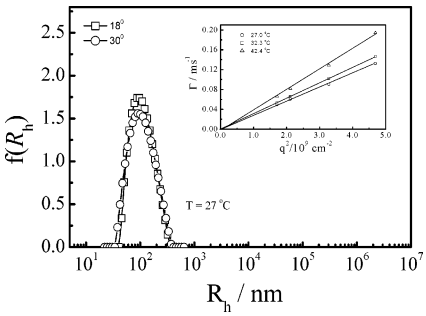

Figure 6. Hydrodynamic radius distribution $f(R_h)$ of multiblock copolymer at two different angles and concentration was 1.0×10^{-6} g/mL. The inset shows q^2 dependence of average line-width Γ of multiblock copolymer chains at different temperature.

lized by the two attached hydrophilic PEO blocks on the chain backbone, resulting in a string−bead chain conformation. On the other hand, Figure 6 shows typical hydrodynamic radius distributions $f(R_h)$ of the multiblock copolymer chains at two different angles at 27 °C, revealing that the size distribution of the copolymer chains is not broad and $\langle R_h \rangle$ is independent of the scattering angle. For such a copolymer, the cumulant analysis of each measured intensity−intensity time correlation function is sufficient for an accurate determination of the average line-width $\langle \Gamma \rangle$. The inset of Figure 6 shows that $\langle \Gamma \rangle$ vs q^2 is a straight line passing through the origin at different temperatures. Each slope leads to one $\langle D \rangle_0$ or further to $\langle R_h \rangle$. The increase of the slope with the solution temperature reflects the increase of $\langle D \rangle_0$, i.e., the decrease of $\langle R_h \rangle$, indicating the contraction of the PNIPAM blocks on each multiblock chain.

Figures 7 and 8 summarize the temperature dependence of $\langle R_g \rangle$, $\langle R_h \rangle$, and $\langle R_g \rangle / \langle R_h \rangle$ of multiblock copolymer chains in water during one heating-and-cooling cycle. Each data point was obtained after the solution reached its temperature equilibrium. It is interesting to find that $\langle R_g \rangle$ remains a constant, but $\langle R_h \rangle$ decreases, as the solution temperature increases. Figures 7 and

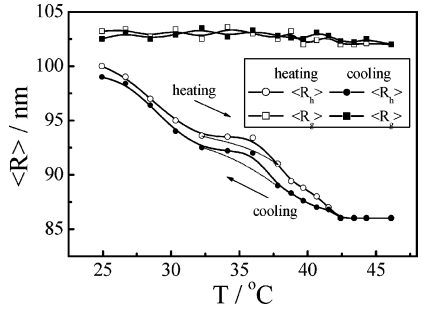

Figure 7. Temperature dependence of z-average of root-mean-square radius of gyration ($\langle R_g \rangle$) and hydrodynamic radius ($\langle R_h \rangle$) of multiblock copolymer chains in water during heating and cooling, where all the symbols and labels have the same meanings as in Figure 5. The concentration was 1.0×10^{-6} g/mL, and the relative error is no more than 2% for each data point.

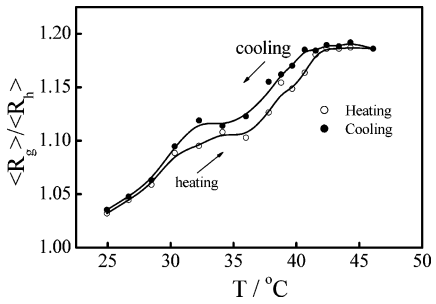

Figure 8. Temperature dependence of ratio of average radius of gyration ($\langle R_g \rangle$) to average hydrodynamic radius ($\langle R_h \rangle$) of multiblock copolymer chains in water during heating and cooling, where all the symbols and labels have the same meanings as in Figure 5. The concentration was 1.0×10^{-6} g/mL, and the relative error is no more than 5% for each data point.

8 can be divided into three temperature regions. In the range 25−32 °C, $\langle R_g \rangle / \langle R_h \rangle$ increases from 1.0 to 1.14. Note that for a random coil chain $\langle R_g \rangle / \langle R_h \rangle \sim 1.5$. The lower value of $\langle R_g \rangle / \langle R_h \rangle$ might be attributed to the existence of many hydrophobic S−S linkages on the chain backbone. They act as hydrophobic "stickers" and make each multiblock chain more compact, like an "ordered coil".[23] On the other hand, for multiblock copolymer chains in a solvent, the swelling degrees or the excluded volumes of different blocks are different even in a good common solvent. One might have to consider ternary interactions. To our knowledge, there has been no existing theory to account for the conformation of a long multiblock copolymer in solution. In the range 32−35 °C, both $\langle R_g \rangle$ and $\langle R_h \rangle$ remain constant, apparently indicating that the chain contraction stops. In the range 35−42 °C, the multiblock copolymer chains start to shrink again before they approach their plateaus, indicating that the PNIPAM blocks in a multiblock copolymer chains are fully collapsed at $T > \sim 42$ °C. Figures 7 and 8 show a hysteresis during the cooling process; namely, $\langle R_h \rangle$ is slightly smaller, especially in the temperature range 30−40 °C, consisting with the hysteresis observed in the coil-to-globule transition of individual PNIPAM homopolymer chains.[13] It has been shown that $\langle R_g \rangle / \langle R_h \rangle$ significantly decreases during the coil-to-globule transition of a PNIPAM homopolymer chain.[13] However, Figure 8 reveals that $\langle R_g \rangle / \langle R_h \rangle$ increases with the solution temperature. Obviously, the increase of $\langle R_g \rangle / \langle R_h \rangle$ is due to the decrease of $\langle R_h \rangle$ because $\langle R_g \rangle$ remains a constant during one heating−cooling cycle. Recently, similar results have also been observed on another multiblock copolymer/solvent system [$(PI$-*b*-$PS)_n$ in cyclohexane], in which $\langle R_g \rangle$ remains a constant and $\langle R_h \rangle$ slightly decreases as the solvent quality becomes poorer.

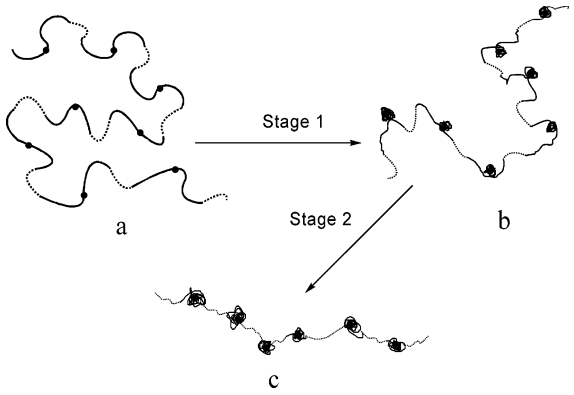

Figure 9. Schematic of the two transition stages of the multiblock copolymer chain in water during heating. The solid lines represent PNIPAM blocks, the broken lines represent PEO blocks, and the black dots represent S−S bonds.

How does one explain such an increase of $\langle R_g \rangle / \langle R_h \rangle$ and the constant $\langle R_g \rangle$ as individual PNIPAM blocks on the chain backbone shrink? Note that for a given system the $\langle R_g \rangle / \langle R_h \rangle$ increases as the chain becomes more extended.[24−30] A rational and simple hand-wave explanation is as follows. As the solution temperature increases, the collapse of each PNIPAM block into a globule (pearl) makes the chain shorter, but at the same time, its two neighboring PEO blocks become less flexible. This leads to a decrease in the number of the Kuhn segments, but an increase in the length of each Kuhn segment. These two opposite effects somehow cancel each other so that $\langle R_g \rangle$ remains a constant.

A more qualitative estimation is as follows: for each PNIPAM block (124 monomer units) in a solvent, the average end-to-end distance (R_0) is about 5 nm, corresponding to a radius of gyration of ∼2 nm. On the other hand, the average diameter of each fully collapsed PNIPAM block, estimated on the basis of its molar mass and chain density in the collapsed state, is about 5−6 nm, corresponding to a radius of gyration of ∼4−5 nm.[13] The collapse of each PNIPAM block leads to microphase separation between PEO and PNIPAM blocks so that the two ends of each PNIPAM block should be pulled out by the two soluble neighboring PEO blocks and stay near the periphery of the PNIPAM globule. It is expected that the contraction of each PNIPAM block would lead to a slight decrease of its end-to-end distance (10−20%). Also note that each initial PEO block (23 monomer units) in the multiblock chain has an average end-to-end distance of ∼2 nm. The formation of individual PNIPAM globules on the copolymer chain at higher temperatures should increase the end-to-end distance of each PEO block because each end is now attached with a 5−6 nm collapsed PNIPAM globule. Our proposed mechanism is indirectly supported by the fact that for the same low copolymer concentration (10^{-5} g/mL) initial triblock copolymer in its solution at higher temperatures start to undergo interchain association to form micelle-like aggregates, but for the multiblock copolymer in its solution, no intrachain and interchain PS association was observed even thought triblock and multiblock copolymer solutions contain the same numbers of PI and PS blocks, i.e., identical chemical composition.

The chain becomes shorter and thicker with a more extended conformation, as schematically shown in Figure 9. The contraction of individual PNIPAM blocks and the overall chain extension have opposite effects on both $\langle R_g \rangle$ and $\langle R_h \rangle$. $\langle R_g \rangle$ is more sensitive to the mass distribution in space. This might explain why $\langle R_g \rangle$ remains a constant and $\langle R_h \rangle$ only decrease ∼5%, much less than the dramatic decrease of both $\langle R_g \rangle$ and $\langle R_h \rangle$ in the collapse of PNIPAM homopolymer chains in water.[13] Since each hydrophobic S−S linkage in the middle connects two PNIPAM blocks, it is expected that the PNIPAM segments around the S−S linkage collapse at a lower temperature than that near the hydrophilic PEO blocks. This can explain the two stages in one heating-and-cooling cycle.

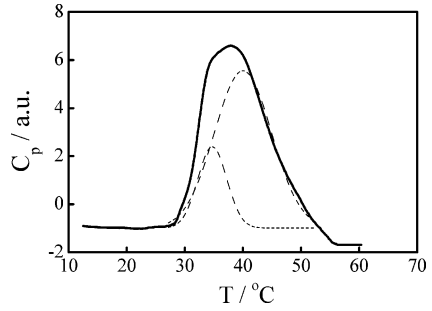

Figure 10. Temperature dependence of partial heat capacity (C_p) of multiblock copolymer chains in water where the heating rate was 1.0 °C/min and the concentration was 1.0×10^{-3} g/mL.

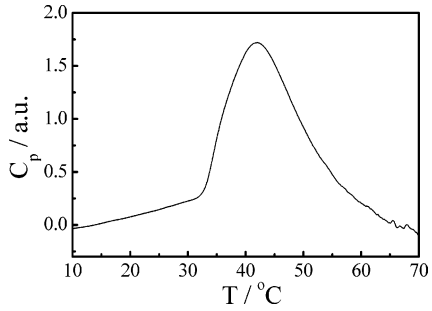

Figure 11. Temperature dependence of partial heat capacity (C_p) of triblock copolymer chains $NC(Me_2)C-PNIPAM_{62}$-*b*-PEO_{23}-*b*-$PNIPAM_{62}-C(Me_2)CN$ in water where the heating rate was 1.0 °C/min and the concentration was 1.0×10^{-3} g/mL.

Tenhu et al.[31] found similar two stages in the collapse of linear PNIPAM homopolymer chains grafted on gold nanoparticles. The two stages were attributed to the sequential collapse of inner and outer PNIPAM segments; i.e., the PNIPAM segments near the gold particle are more hydrophobic so that they collapse at a lower temperature. Tenhu et al.[32] also studied the association of diblock PEO-*b*-PNIPAM chains in an aqueous solution at higher temperatures and found that increasing the PEO length can critically affect the size of resultant aggregates because a long PEO block can stabilize more collapsed PNIPAM segments. In addition, the hydrophilic PEO block shifts the LCST of PNIPAM segments from ∼32 to ∼36 °C.

Association of Multiblock and Triblock Copolymer Chains. The concentrations used in the association study were relatively concentrated (1.0×10^{-3} g/mL). First, the partial heat capacities (C_p) respectively involved in the association of multiblock and triblock copolymer chains without trithiocarbonate ends in aqueous solutions was measured using the Micro-DSC. Figure 10 shows that in the heating process there are two peaks located at ∼33 and ∼41 °C for multiblock copolymer chains. In contrast, Figure 11 shows that for triblock copolymer chains only one broad peak enters at ∼41 °C, resembling the higher temperature peak in Figure 10.

Figure 12 shows the temperature dependence of the average aggregation number (N_{agg}) for both triblock and multiblock copolymer chains in aqueous solutions. The multiblock copolymer chains start to associate at ∼33 °C, corresponding to the first peak in Figure 10. After the solution temperature reaches ∼36 °C, the interchain association stops and only 5−6 chains aggregate together. Further increase of both $\langle R_h \rangle$ and $\langle R_g \rangle$ at

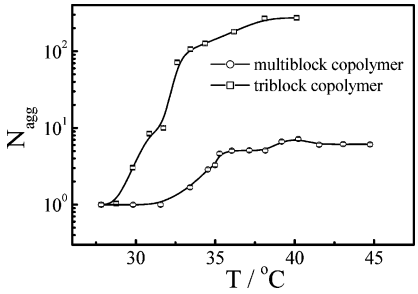

Figure 12. Aggregation number of multiblock copolymer and triblock copolymer chains as a function of the temperature at the concentration of 1.0×10^{-3} g/mL, where the relative error is no more than 8% for each data point.

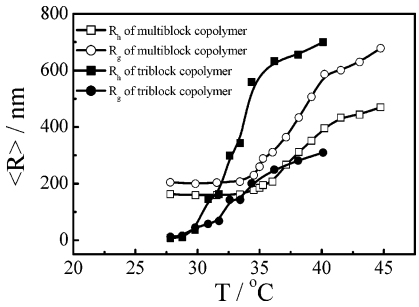

Figure 13. Temperature dependence of *z*-average of root-mean-square radius of gyration ($\langle R_g \rangle$) and hydrodynamic radius ($\langle R_h \rangle$) of multi- and triblock copolymer chains in water during heating, where all the symbols and labels have the same meanings as in Figure 12. The concentration was 1.0×10^{-3} g/mL, where the relative errors of $\langle R_g \rangle$ and $\langle R_h \rangle$ are no more than 5% and 2% for each data point, respectively.

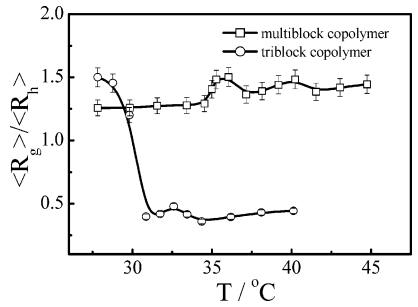

Figure 14. Temperature dependence of ratio of average radius of gyration ($\langle R_g \rangle$) to average hydrodynamic radius ($\langle R_h \rangle$) of multi- and triblock copolymer chains in water during heating process, where all the symbols and labels have the same meanings as in Figure 12. The concentration was 1.0×10^{-3} g/mL, where the relative errors of $\langle R_g \rangle$ and $\langle R_h \rangle$ are no more than 5% and 2% for each data point, respectively.

higher temperatures, as shown in Figure 13, is due to the chain extension as we observed in the single-chain folding. On the other hand, Figure 12 shows that for the triblock copolymer chains N_{agg} continuously increases with the temperature, starting at ~30 °C. This explains why we observed only one broad peak in Figure 11.

Figure 14 shows an expected decrease of $\langle R_g \rangle / \langle R_h \rangle$ for triblock chains because the interchain association of the PNIPAM blocks leads to the formation of spherical polymeric micelles. It has been known that for a uniform and hard sphere $\langle R_g \rangle / \langle R_h \rangle \sim 0.774$.[13] Lower value of $\langle R_g \rangle / \langle R_h \rangle$ reflects that the polymeric micelles have a less-dense periphery.[24−30] For multiblock chains, the increase of $\langle R_g \rangle / \langle R_h \rangle$ is due to the chain extension in the range 33−36 °C. It should be stated that interchain association of PNIPAM homopolymer and copolymer chains in solutions has been extensively studied. Previous results reveal that it is rather difficult to cleanly separate interchain association and intrachain contraction as the solution temperature increases. Note

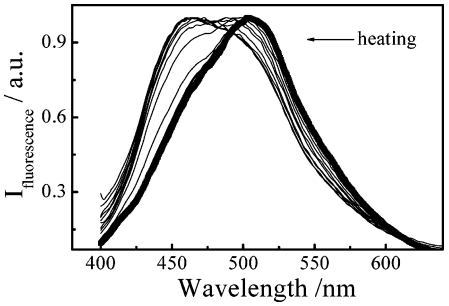

Figure 15. Fluorescence spectra of multiblock copolymer at different temperatures and the concentration was 1.0×10^{-3} g/mL.

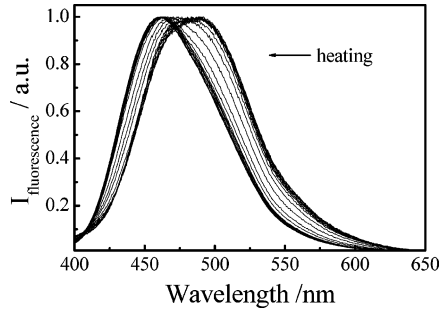

Figure 16. Fluorescence spectra of triblock copolymer $NC(Me_2)C-PNIPAM_{62}$-*b*-PEO_{23}-*b*-$PNIPAM_{62}-C(Me_2)CN$ at different temperatures, and the concentration was 1.0×10^{-3} g/mL.

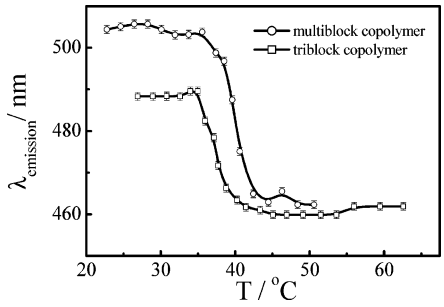

Figure 17. Fluorescence wavelength of multi- and triblock copolymer as a function of temperature, and the concentration was 1.0×10^{-3} g/mL.

that our multiblock and triblock copolymer chains have an identical chemical composition. The existence of hydrophilic and soluble PEO segments prevents the collapse of each multiblock copolymer chain into a single-chain globule. The collapse of the PNIPAM blocks leads to the formation of individual small globules (beads) on the chain backbone so that the multiblock chain becomes thicker and more extended.

Figures 15 and 16 show the temperature dependence of normalized fluorescence spectra of *N*-phenyl-α-naphthylamine (PNA, a fluorescence probe), respectively, in aqueous solutions of multiblock and triblock copolymers, where C_{PNA} is 10 μM. It has been known that PNA strongly emits fluorescence in a nonpolar solvent or within a hydrophobic microenvironment, but fluorescence is quenched in a polar media.[33] A comparison of Figures 13−17 shows that the multiblock copolymer chains start to contract at ~32 °C, but they associate at ~36 °C, reflecting in the decrease of $\lambda_{emission}$. In contrast, the triblock copolymer chains start to associate at a lower temperature.

Conclusion

Thermally sensitive long multiblock copolymer (PEO_{23}-*b*-$PNIPAM_{124})_n$ with $n = 750$ can be synthesized via the coupling reaction between two SH end groups of triblock copolymer

chains HS−PNIPAM$_{62}$-*b*-PEO$_{23}$-*b*-PNIPAM$_{62}$−SH. The study of the single-chain folding in an extremely dilute solution shows that the PNIPAM segments near the PEO blocks and in the middle near the S−S linkages collapse at two different temperatures, resulting in two stages during the heating process. Consequently, the association of multiblock chains in a relative more concentrated solution also has two stages. Our results reveal that in the heating process the contraction of individual PNIPAM blocks leads no interblock aggregation. Instead, each multiblock copolymer chain becomes shorter and thicker with a more extend conformation. Therefore, its radius of gyration remains a constant and its hydrodynamic radius only slightly decreases. In contrast, the association of triblock copolymer chains NC(Me$_2$)C−PNIPAM$_{62}$-*b*-PEO$_{23}$-*b*-PNIPAM$_{62}$−C(Me$_2$)-CN occurs at ∼30 °C, resulting in an expected micellar structure.

Acknowledgment. This work was supported by the Shanghai-Hong Kong Joint Laboratory in Chemical Synthesis, the CAS Special Grant (KJCX2-SW-H14), the NNSFC Projects (20534020 and 20574065), the Hong Kong Special Administration Region Earmarked Project (CUHK4037/06P, 2160298), and NSFC/RGC Joint Research Scheme (20710011 and N_CUHK446/06). Z.Q. thanks the Croucher Studentship.

References and Notes

(1) Grosberg, A. Y.; Khokhlov, A. R. *Adv. Polym. Sci.* **2006**, *196*, 189.
(2) Zhang, G.; Wu, C. *Adv. Polym. Sci.* **2006**, *195*, 101.
(3) Stryer, L. *Biochemistry*; W.H. Freeman: New York, 1988.
(4) Khokhlov, A. R.; Khalatur, P. G. *Phys. Rev. Lett.* **1999**, *82*, 3456.
(5) Timoshenko, E. G.; Kuznetsov, Y. A. *J. Chem. Phys.* **2000**, *112*, 8163.
(6) Khokhlov, A. R.; Berezkin, A. V.; Khalatur, P. G. *J. Polym. Sci., Part A: Polym. Chem.* **2004**, *42*, 5339.
(7) Lozinsky, V. I. *Adv. Polym. Sci.* **2006**, *196*, 87.
(8) Virtanen, J.; Baron, C.; Tenhu, H. *Macromolecules* **2000**, *33*, 336.
(9) Wahlund, P. O.; Galaev, I. Y.; Kazakov, S. A.; Lozinsky, V. I.; Mattiasson, B. *Macromol. Biosci.* **2002**, *2*, 33.
(10) Nissen, P.; Hansen, J.; Ban, N.; Moore, P. B.; Steitz, T. A. *Science* **2000**, *289*, 920.
(11) Hodge, P.; Sherrington, D. C. *Polymer-Supported Reactions in Organic Synthesis;* Wiley: New York, 1980.
(12) Burgess, K. *Solid-Phase Organic Synthesis;* Wiley: New York, 2000.
(13) Wu, C.; Zhou, S. Q. *Macromolecules* **1995**, *28*, 8381.
(14) Tiktopulo, E. I.; Bychkova, V. E.; Ricka, J.; Ptitsyn, O. B. *Macromolecules* **1994**, *27*, 2879.
(15) Chiefari, J.; Chong, Y. K.; Ercole, F.; Kristina, J.; Jeffery, J.; Le, T. P. T.; Mayadunne, R. T. A.; Meijs, G. F.; Moad, C. L.; Moad, G.; Rizzardo, E.; Thang, S. H. *Macromolecules* **1998**, *31*, 5559.
(16) Mayadunne, R. T. A.; Rizzardo, E.; Chiefari, J.; Kristina, J.; Moad, C. L.; Postma, A.; Thang, S. H. *Macromolecules* **2000**, *33*, 243.
(17) Lai, J. T.; Filla, D.; Shea, R. *Macromolecules* **2002**, *35*, 6754.
(18) Chu, B. *Laser Light Scattering*, 2nd ed.; Academic Press: New York, 1991.
(19) Berne, B. J.; Pecora, R. *Dynamic Light Scattering*; Plenum Press: New York, 1976.
(20) Hong, C.-Y.; You, Y-Z.; Pan, C.-Y. *J. Polym. Sci., Part A: Polym. Chem.* **2004**, *42*, 4873.
(21) (a) Perrier, S.; Takolpuckdee, P.; Mars, C. A. *Macromolecules* **2005**, *38*, 2033. (b) Mayadunne, R. T. A.; Rizzardo, E.; Chiefari, J.; Krstina, J.; Moad, G.; Postma, A.; Thang, S. H. *Macromolecules* **2000**, *33*, 243.
(22) Qiu, X. P.; Winnik, F. M. *Macromolecules* **2007**, *40*, 872.
(23) Halperin, A. *Macromolecules* **1991**, *24*, 1418.
(24) Wu, C.; Qiu, X. P. *Phy. Rev. Lett.* **1998**, *80*, 620.
(25) Li, X. Y.; He, X.; Ng, A. C. H.; Ng, D.; Ng, T.; Wu, C. *Macromolecules* **2000**, *33*, 2119.
(26) Siu, M.; Zhang, G. Z.; Wu, C. *Macromolecules* **2002**, *35*, 2723.
(27) Wang, X. H.; Goh, S. H.; Lu, Z. H.; Wu, C. *Macromolecules* **1999**, *32*, 2786.
(28) Wu, C.; Zhou, S. Q.; Wang, W. *Biopolymers* **1995**, *35*, 385.
(29) Hu, T. J.; You, Y. Z.; Pan, C. Y.; Wu, C. *J. Phys. Chem. B* **2002**, *106*, 6659.
(30) Siu, M.; Liu, H. Y.; Zhu, X. X.; Wu, C. *Macromolecules* **2003**, *36*, 2103.
(31) Shan, J.; Chen, J.; Nuopponen, M.; Tenhu, H. *Langmiur* **2004**, *20*, 4671.
(32) Virtanen, J.; Holappa, S.; Lemmetyinen, H.; Tenhu, H. *Macromolecules* **2002**, *35*, 4736.
(33) Mcclure, W. O.; Edelman, G. M. *Biochemistry* **1966**, *5*, 1908.

MA702139B